J. Fluid Mech. (1968), *vol.* 31, *part* 1, *pp.* 1–15
Printed in Great Britain

Evolution of two-dimensional periodic Rayleigh convection cells of arbitrary wave-numbers

By MICHAEL M. CHEN AND JOHN A. WHITEHEAD
Yale University, New Haven, Connecticut

(Received 8 June 1967)

By introducing small controlled perturbations prior to the onset of motion, two-dimensional convection cells of arbitrary width–depth ratios are produced in a horizontal fluid layer heated from below. The conditions employed correspond to the finite-amplitude Rayleigh stability problem for a constant viscosity, large Prandtl number, Boussinesq fluid with rigid, conducting boundaries. It was found that two-dimensional cells with width–depth ratios close to unity are stable at all Rayleigh numbers investigated ($R_c \leqslant R \leqslant 2{\cdot}5R_c$). Cells whose width–depth ratios are moderately too large or too small tend to undergo size adjustments toward a preferred value of about 1·1. If the width–depth ratios are much too large or too small, they tend to develop three-dimensional instabilities in the form of cell boundary distortions and transverse secondary cells, respectively. Eventually the flow settles into a new family of rolls with a more preferred width–depth ratio. It is suggested that these observations may have implications on nonlinear interchange instability problems and geophysical flows.

1. Introduction

When the vertical temperature gradient of a fluid layer heated from below exceeds a critical magnitude, the motionless state is known to be unstable and buoyancy-generated convection motion must exist. The onset of such flows, known as the Rayleigh stability problem, has been thoroughly studied experimentally and theoretically. A relatively recent survey was given by Chandrasekhar (1961). The present communication describes an experiment designed to examine some qualitative aspects of such convection, particularly with respect to the band-width of finite-amplitude steady-state modes which could be maintained at moderately supercritical conditions.

The study has been motivated by several considerations. Thermal convection is the simplest member of a large family of hydrodynamic and hydromagnetic flows arising out of interchange instabilities. While the onset of motion is generally well understood in terms of linear stability theories, current understanding of finite-amplitude supercritical flows is quite sketchy. One of the basic questions is what modes can be expected to exist in finite-amplitude flows, and whether the expected modes bear any relationship to the linear modes. A somewhat related problem is the nature of the interaction between finite-amplitude modes. These problems are theoretically difficult, due to the inherently nonlinear nature of the governing equations. One would thus hope that a detailed experimental

observation of the thermal convection problem may offer useful insight into the more complex problems.

A long-standing problem concerning thermal convection is the basic structure of the finite-amplitude flow, i.e. whether the cells are regular hexagons, irregular granules, or other shapes. Probably as a result of the beautiful photographs of Bénard (1901), after whom the cells are now named, for many years thermal convection had been associated with hexagonal cells. Recent theoretical studies (Segel 1965; Schlüter, Lortz & Busse 1965) and qualitative experimental evidence (Chen 1966; Koschmieder 1966) on the other hand indicate that the cell structure depends on many factors. but should be primarily two-dimensional for the basic Rayleigh convection problem with negligible or moderate (say $\leqslant 20\,\%$) viscosity variations. Solutions for such steady two-dimensional flows for critical wave-number or arbitrary wave-numbers have been given by Malkus & Veronis (1958), Kuo (1961), Veronis (1966) and Fromm (1965), among others. The present experiments explore the range of conditions and wave-numbers which can result in stable two-dimensional cellular flows.

Lastly, regularly arranged long vortices are frequently found in meteorology and oceanography. Some of these are known to be thermal in origin. It is reasonable to expect that the size of these vortices is related to a certain characteristic depth of the unstable thermal layer. One might then inquire how these vortices would respond to climatic or seasonal changes which alter the depth of this thermal layer. The problem being investigated here is, in a qualitative way, a simple laboratory prototype of the more complex geophysical problem.

It is clear that conventional convection experiments provide only incomplete information on the behaviour of finite-amplitude cells. These experiments usually begin with a motionless, subcritical condition. As the temperature difference is increased above the critical value, cellular convection gradually develops. Consequently, the observed finite-amplitude modes, at least in the earlier stages, correspond closely to the linear modes which have the fastest growth rates at convection onset. This is shown schematically as the loci A in figure 1. Such experiments have two shortcomings. Variations in starting procedures may result in different time-dependent temperature profiles at convection onset, and hence correspondingly different finite-amplitude modes. This can be seen by the drastically different structures between the slow experiments of Koschmieder (1966) and the fast experiments of Chen (1966) and Krishnamurti (1967). Another disadvantage is that since the procedure favours the faster-growing linear modes there may be a class or band of stable nonlinear modes which could escape detection in the laboratory, simply because their infinitesimal modes grow slowly.

One way to overcome this difficulty, suggested by Chen (1966), is to create convection cells corresponding to certain chosen modes, and then study their subsequent evolution. By exploring all important modes, a relatively complete picture can be formed. The actual technique involves the introduction of temporary external excitations of the chosen mode before the temperature difference reaches the critical value, as shown by loci B in figure 1. In this manner, the mode corresponding to the artificial perturbation has a clear amplitude advantage

over the other modes of possible perturbations when supercritical conditions are reached. If this advantage is sufficiently large, subsequent nonlinear interaction may tend to inhibit other modes, allowing only the chosen mode to continue its growth. At this time, the artificial perturbation can be removed so that the flow will settle into a steady-state configuration without the influence of the extraneous perturbations.

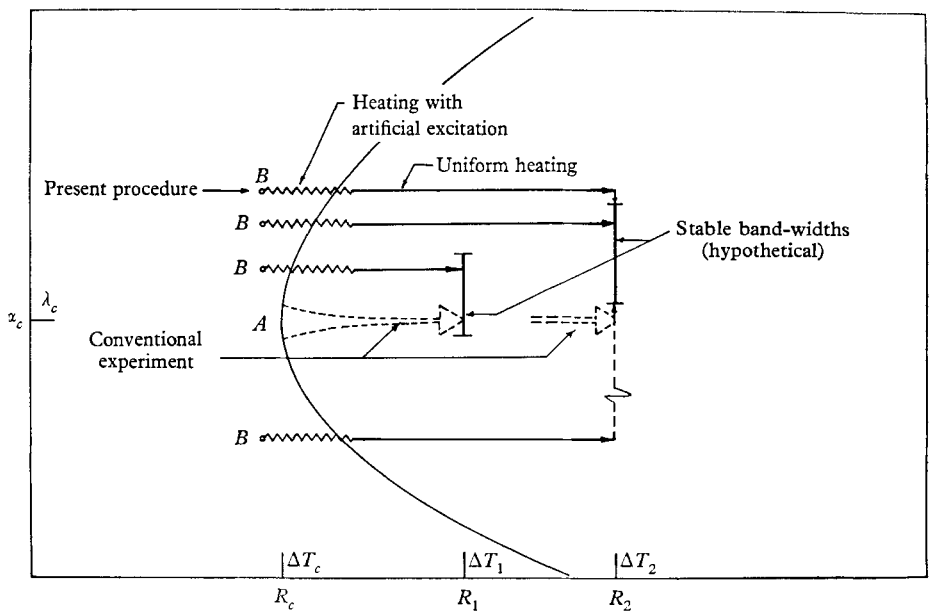

FIGURE 1. Comparison of conventional experiments in convection, shown by loci *A*, and the present technique, shown by loci *B*.

In the present experiments, the artificial starting perturbations were in the form of non-uniform thermal radiation. They were produced by passing the output of an incandescent heat lamp through a metal template, cut in a pattern corresponding to the mode to be excited (see figure 2, plate 1, and figure 3). The radiation, rich in infra-red, subsequently passed though the relatively transparent top cooling jacket, and was absorbed by the fluid layer under investigation, which was somewhat more opaque to the infra-red radiation. The shadows of the template thus produce the non-uniform heating pattern in the fluid layer. Since the present study is primarily concerned with roll cells, the templates consisted of gratings of different spacings, as shown in figure 2, plate 1. In all cases, satisfactory cell structure can be generated with very short durations of perturbing radiation (less than $0{\cdot}2h^2/a$: see discussion on dimensionless time in §3) and very low perturbing power levels ($< 1\,\%$ the net heat transfer rate between the two plates).

As it was our intention to study the most basic features of the problem, we chose to study the simplest possible system which could be established in the laboratory. The fluid layer under investigation was confined between two hori-

zontal solid surfaces to avoid surface tension and other uncertainties associated with free-surface experiments. The temperature difference was kept low to keep the viscosity variation below 5 %. The experiment thus approaches the theoretical model of constant property Boussinesq approximation with rigid, perfectly conducting boundaries. Departures from the last stated condition, however, could not be completely eliminated, and will be discussed in detail later.

2. Experimental details

The apparatus

The design of the experimental apparatus is faced with many conflicting requirements. For example, visualization considerations made it desirable to use transparent materials for the top plate. The relatively low thermal conductivity of glasses (about 5–7 times that of oil) thus constitutes a less than perfect approximation to the perfectly conducting boundary condition preferable on theoretical grounds. The use of a thick aluminium or copper plate was desirable to enhance the uniformity of bottom surface temperature, but would also increase the thermal mass, which was undesirable as will be discussed later. The location of temperature sensors pose another problem, for if they were placed on the glass, where they would yield the most accurate results, they would surely influence the cell structure.

The apparatus, which is a compromise of these and other requirements, is shown in figure 3. The depths of the fluid layer used were $\frac{3}{8}$ in., $\frac{1}{2}$ in., and $\frac{5}{8}$ in. A $\frac{1}{8}$ in. glass mirror was placed under the fluid layer to form the bottom surface. The mirror was part of the shadowgraph visualization arrangement. A $\frac{1}{4}$ in. aluminium plate was placed immediately below the glass to provide a uniform bottom temperature. Iron–constantan thermocouples were placed on the underside of this aluminium plate.

The working fluid was silicon oil (Dow Corning 200 fluid). Several grades were mixed to give a viscosity which required no more than 4 degC temperature difference at critical Rayleigh number. For the layer depths chosen, this corresponded to a kinematic viscosity range of between 1 and 5 cm^2/sec with less than 5 % difference between the viscosities at the top and the bottom of the layer.

The heater consisted of a $\frac{1}{4}$ in. aluminium plate with nichrome wires fibreglassed to the underside. The nichrome wires were arranged approximately $\frac{3}{16}$ in. apart. It has been estimated from heat conduction equations that at the bottom oil surface the non-uniformities caused by the spacing of the nichrome wires would be completely negligible (10^{-16} degC) compared to natural thermal fluctuations in the material. A radial temperature difference, however, could not be completely eliminated, probably due to heat loss from the sides. This amounted to 0·1 degC when total temperature difference was approximately 5 degC. A careful examination of the experimental results indicated that this had very little effect on the conclusions drawn. The heater was powered by a zener shunted d.c. power supply which kept the supply voltage fluctuations to well within 1 %.

The fluid layer was cooled on top by a transparent water jacket. Two separate water jackets were used. The first water jacket consisted of a $\frac{3}{4}$ in. top plate made of plexiglass and a $\frac{1}{4}$ in. bottom plate made of plate glass. In the course of

the experiments, it was found that the plexiglass caused some optical distortion, probably due to combined influences of radiation heating and hygroscopic absorption. A new water jacket was then made with a $\frac{1}{2}$ in. glass plate used in place of the plexiglass. The photographs in this communication were made with the all-glass water jacket. The flow rate in the water jacket was maintained at sufficient level to reduce the temperature drop to insignificant values.

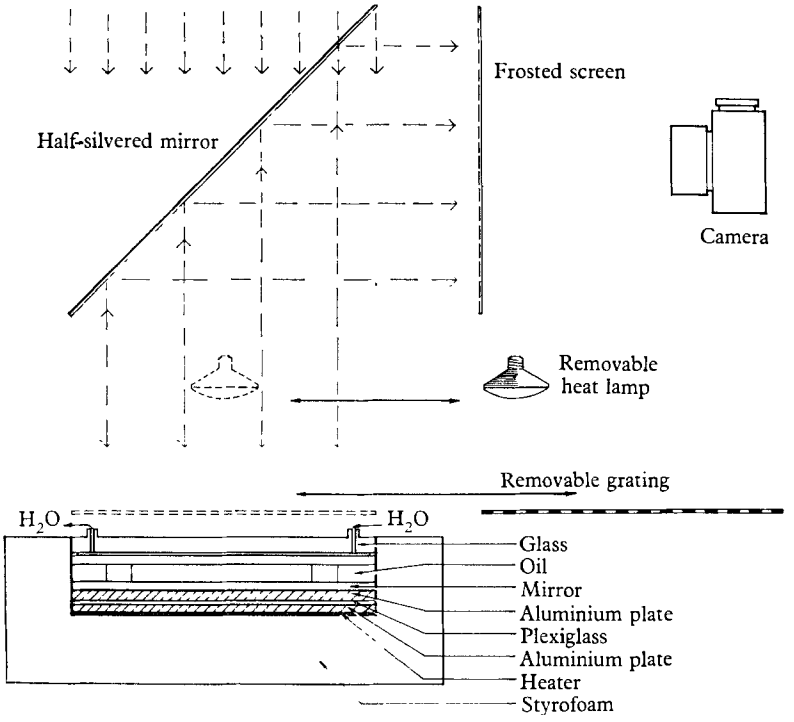

FIGURE 3. Schematic diagram of the experimental apparatus.

Based on measured thermophysical properties of glass it was estimated that at subcritical Rayleigh numbers the two layers of glass constitute a total of approximately 10 % of the total heat transfer resistance between the aluminium plate and the water. An additional 1 % or less was contributed by the cooling water. The influence of this on convection onset will be discussed in §4. In principle, it would be possible to reduce these resistances to smaller fractions of the total by using a thicker oil layer or by using thinner glass. In practice, the former alternative would require the use of a much larger apparatus in order to reduce edge effects, whereas the latter alternative would result in a loss of rigidity for the glass, resulting in sagging in the centre. The cell structure at convection onset appears to be strongly influenced by even a minute amount of sag. In the present apparatus the pressure of the oil and cooling water was also carefully balanced to reduce this sag.

In view of the low heat transfer rate involved, the entire apparatus was carefully insulated with 2 in. of Styrofoam; in addition, the room temperature was controlled to within 0·2 degC of the temperature of the cooling water. These

precautions were taken to ensure constant conditions during the long runs which were necessary in view of the long time constants involved. No attempt was made to obtain an experimental heat balance for the experiments.

After preliminary experiments indicated that some linear roll cells tend to degenerate into rolls of different orientations, an effort was made to eliminate all possible influences which might affect the natural selection of cell orientations. A circular plexiglass ring of 12 in. I.D. was introduced in the fluid layer to simplify the geometry of the horizontal boundary. The inside of this ring was the actual extent photographed in figures 5, 7, 8, 9, 10 (plates 2–6).

The radiation source used to excite the desired mode consisted of a commercial incandescent heat lamp rated at 600 W. It was operated at a reduced power at 400 W through a variac. In order to prevent interference with visualization, both the heat lamp and the grating were normally stored outside of the optical path of the shadowgraph, and only brought into position briefly during the start of the experiment. Based on the estimated absorption characteristics of glass, water and silicone oil, it was estimated that the actual perturbing power was less than 1 W. Since the heat lamp was never left on for more than several minutes, the total energy absorbed by the oil layer was of the order of 10^2 to 10^3 joules.

The fixed gratings, shown in figure 2, consisted of $\frac{1}{4}$ in. $\times$ 12 in. $\times$ 12 in. aluminium plates with milled open slots. The spacings between the slots were equal to the slot width, the sum of the spacing and the slot width being equal to twice the desired cell size, with a small correction to account for the diverging rays. The resulting radiation intensity thus corresponds to a square wave pattern. While the pattern is clearly rich in higher harmonics, these did not seem to affect the finite-amplitude cells produced. The only second harmonic observed (see figure 10) had a different phase relationship from that expected of a square wave. The variable gratings had adjustable slots. Care was taken to keep the slot width and the spacing approximately equal, although there was no evidence that this is important.

The shadowgraph consisted of a light source placed sufficiently far to provide a nearly parallel light which passed through the convecting layer twice before reaching a rear projection screen, where it was observed and photographed. Due to the temperature dependence of the refractive index of the oil, light beams were bent toward the low-temperature zones-forming bright lines at low, temperature cell boundaries.

Since optical quality mirrors of the sizes required would be prohibitively expensive, the mirrors were of the best commercial grade. These mirrors caused some optical distortions, making the circle appear slightly out of round. The cell size measurements, however, have taken this into consideration. The uncertainty on the cell sizes due to this distortion is considerably smaller than that due to the inherent non-uniformity and irregularity of the cells themselves.

Procedure

In order to avoid uncertainties in the interpretation of stability observations, it is desirable that the time required for the convective flow to reach 'steady state' (i.e. flow corresponding to solutions of nonlinear time-independent

Boussinesq equations) should be short compared to the time constants associated with the instability under investigation. Unfortunately, the aluminium plates used to ensure uniform boundary temperature also greatly added to the heat capacity and the thermal inertia of the system. As a result, it was necessary

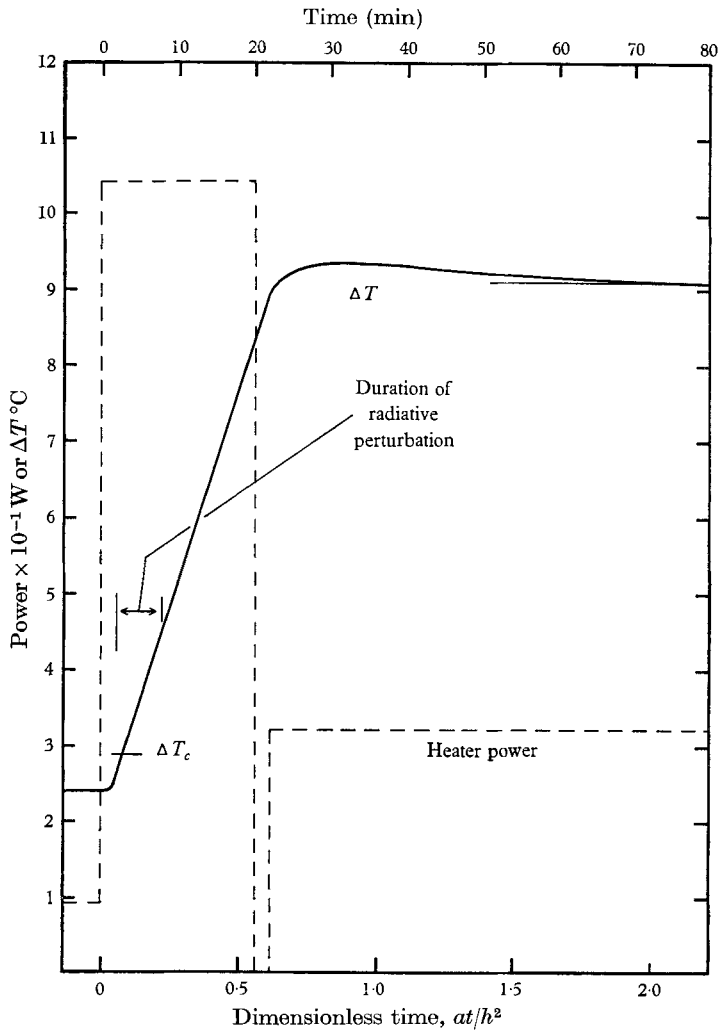

FIGURE 4. Typical heating curve indicating the starting procedure used in the experiments.

to use very large electric power in the beginning to hasten the approach to steady-state temperature differences. A typical heating curve and related events are shown in figure 4. It is seen that the steady-state ΔT could be reached in roughly half an hour.

When desired, the radiative perturbation was turned on just before the ΔT reached the critical value and was turned off about 6–8 min afterwards. This was usually sufficient to allow the unstable feedback mechanism of convection to take over, resulting in flow patterns corresponding closely to the imposed cell

size. Thus, the radiation was only used to trigger the transition to the desired mode. It was never used to maintain convection in this mode.

The calculated thermal time constant for the oil layer with fixed boundary temperatures (see below) was of the order of 3 min. Due to the large Prandtl number the time constant corresponding to the establishment of steady flow is roughly of this order. Therefore, about 15 min after the desired temperature difference is reached, the flow field could be considered to correspond closely to the 'steady-state' flow field for the relevant cell size (except for departures corresponding to unstable modes). Instabilities observed after this time can then be ascribed to the steady-state, finite-amplitude flow of the corresponding cell size with little error.

As soon as the radiation perturbation was turned off, the template was moved out of the way so that shadowgraph pictures could be taken. The shadowgraph screen together with an electric clock and a microammeter arranged to indicate the ΔT between the aluminum plate and the cooling water were photographed at regular intervals with a motor-driven 35 mm camera.

3. Experimental results

Two separate series of experiments are presented here. The first series employed a fluid layer depth of $\frac{1}{2}$ in. and kinematic viscosity of 4·0 cm^2/sec, yielding an experimental critical temperature difference of 3·62 degC. The second series had a layer thickness of $\frac{5}{8}$ in. and viscosity about 4·75 cm^2/sec, yielding an experimental ΔT_c of 2·41 degC. The Prandtl numbers were 998 and 1180 respectively. The viscosity variation at ΔT_c due to the top and bottom temperature difference was always below 2·5 %. Thus the experiments could be considered to correspond to infinite Prandtl number, constant viscosity, Boussinesq flow confined between non-slip conducting boundaries.

Since the experiments for $\frac{1}{2}$ in. thickness employed the plexiglass–glass water jacket, the photographs were subjected to some optical distortion. Consequently only the photographs from the $\frac{5}{8}$ in. series are shown here. However, there were no detectable differences between the results of these series, and the data from both series were included in the stability map in figure 11.

A preliminary series of experiments was also conducted with a $\frac{3}{8}$ in. fluid depth. While qualitative observations were consistent with the other two series, the experiments were quite crude and little quantitative data were taken.

In order to avoid theoretical corrections for the critical Rayleigh numbers due to the glass layers, the experimental data were referred to in terms of R/R_c, where R_c indicates the experimentally determined critical Rayleigh number. This was done by plotting the observed temperature difference versus the heat input, and obtaining the point at which the slope changes, similar to the method used by Schmidt & Milverton (1935). Using crudely measured values of the viscosity and thermal conductivity, computed critical ΔT's were found to be within 10 % of the observed values.

The time in the figures is shown in hours and minutes as well as in dimensionless time at/h^2, where a is the thermometric conductivity with the units of

diffusivity and h is the fluid layer thickness. In particular, for the experiments with $h = \frac{5}{8}$ in., one has $h^2/a = 36$ min.

The conduction thermal time constant for flat layers with fixed boundary temperatures is equal to $h^2/\pi^2 a$.

Linear roll cells of moderate sizes

The evolution of roll cells of moderate width-to-depth ratios is shown in figure 5, plate 2. It is seen that basically these cells were structurally stable. It is interesting to note, however, that the larger and smaller cells exhibited some tendencies to adjust the dimensions toward an intermediate value. Since the boundary in the horizontal extent is fixed, this occasionally necessitated the elimination

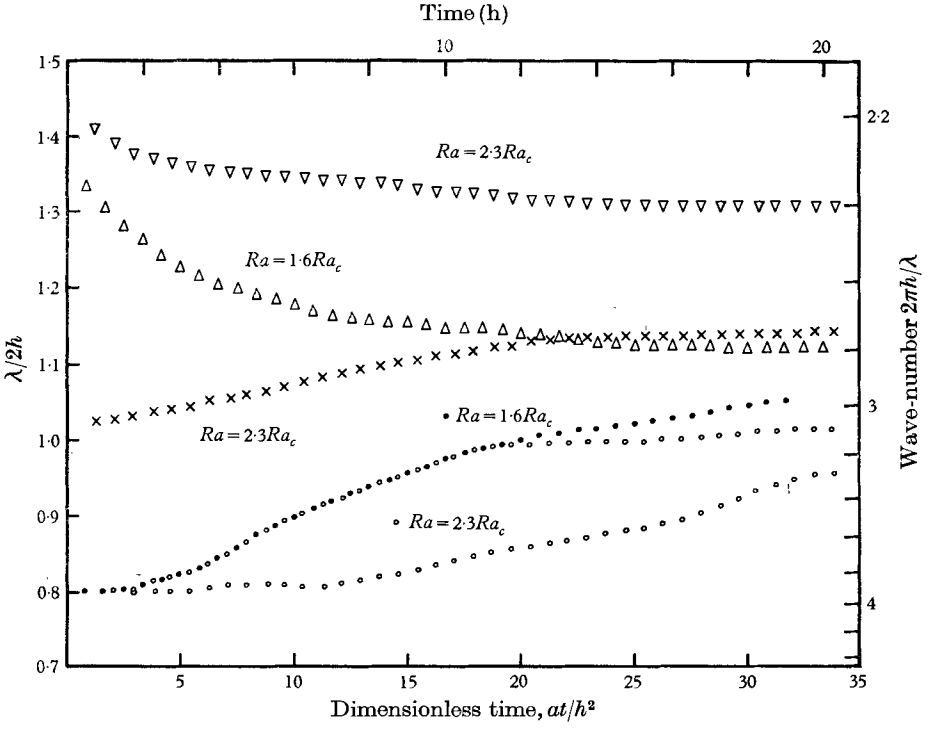

FIGURE 6. Typical plot of roll width-to-depth ratio versus time. This data can only be interpreted qualitatively, as roll sizes are rarely uniform throughout the fluid. The two curves marked with open circles are measured from two different regions in the same experiment, the bottom curve being for a region at the centre, and the top curve being for a region about 3 in. from the centre.

of existing edge cells when the initial cell sizes were too small, as well as the generation of new edge cells when the initial cell sizes were too large. The final width-to-depth ratios were measured and shown as the shaded region in figure 11. These showed considerable scatter, but the fact that convective cells had considerable ability to adjust their dimensions toward a more preferable value was quite obvious.

If one disregards the small imperfections in the cell structure, the above-described flow phenomena can be considered basically two-dimensional. A plot of the cell size or wave-number versus time for several initial cell sizes is shown in figure 6. The curves must be considered semi-quantitative, due to the irregularity of cells. The time constant associated with these cell-size adjustments appears to be of the order of tens of hours, or roughly an order longer than h^2/a.

Excessively small roll cells

An interesting phenomenon occurs when cells were produced with width–depth ratio much smaller than the preferred value. This is shown in figure 7, plate 3. In this case, the cell boundary appears to remain straight, but three-dimensional tertiary flows in the form of subcells tended to develop within these long two-dimensional roll cells. These tertiary flows appeared to be well correlated with those in adjacent rolls, so that, when they attained sufficient amplitude, the convective patterns would take on a rectangular cell pattern. The characteristic widths of these cross-cells, however, were somewhat closer to the preferred aspect ratio.

If the original rolls were sufficiently far from the preferred aspect ratio, in time the secondary cells would dominate and completely swamp the original cell patterns, resulting in roll cells perpendicular to the originally induced ones. These secondary cells have a width–depth ratio closer to the preferred values. In order to indicate that the perpendicular rolls are not the results of systematic non-uniformities in the apparatus, experiments were carried out with the initial rolls in horizontal, diagonal, as well as vertical directions as shown in figure 8, plate 4. In all these cases the metamorphoses were always into cells perpendicular to the original ones.

Excessively large roll cells

When the width-to-depth ratio is much larger than the preferred value, an additional form of three-dimensional instability could be observed. As shown in figure 9, plate 5, this instability was characterized by an apparent lack of rigidity in the cell boundary. Occasionally the boundary may develop a significant amount of zigzagging, even to the point of changing temporarily to an apparent polygonal cell structure. Such polygonal cells, however, invariabily reverted back to roll cells of a more favourable size in a short time.

In some instances, secondary cross-cells of the type described previously in §2 were also found.

The appearance of these cross-cells for large width-to-depth ratios was sometimes attributable to the following mechanism: when the cell size was too large, the second harmonic mode of the original roll cell (i.e. cell width $\lambda_1 = \frac{1}{2}\lambda_0$) may become excited, as shown in figure 10, plate 6. As these smaller rolls gradually 'grow' into prominence they may develop cross-cell instabilities which would then act as finite perturbations to 'reproduce themselves' in the remaining areas. It is not clear, however, whether this explanation could explain all appearances of cross-cell instability in large aspect ratio rolls.

Stability map

The fundamentally different behaviour of the excessively small roll cells as compared to those of modest size suggested that there might exist a critical width-to-depth ratio, below which the flow becomes three-dimensionally unstable. One would further expect that this critical width-to-depth ratio, when plotted as a function of Rayleigh number, would form a neutral stability line on the cell size/Rayleigh number map. In other words, the instability growth rate tends to zero as one approaches this line from below, resulting in ever increasing time

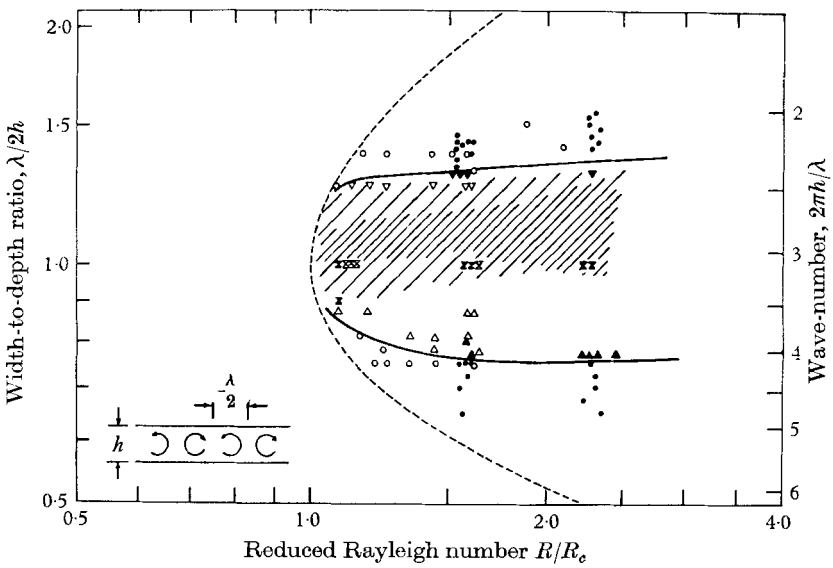

FIGURE 11. Summary of stability observations as functions of roll cell size and Rayleigh number. The open and closed symbols represent results using $\frac{1}{2}$ in. and $\frac{5}{8}$ in. depths, respectively. The lightly shaded region represents the spread of cell sizes at the end of the tests. The heavily shaded region represents the spread of the average cell sizes at the end of each test. The solid lines indicate experimental neutral lines for three-dimensional instabilities. For comparison, the neutral curve for convection onset from linear theory is shown as the dashed line. ▲ △, tending to expand; ▼ ▽, tending to shrink; ● ○, three-dimensional unstable; ⧗ ×, apparently stable.

constants associated with the development of cross-cells. The photographs in figure 7, plate 3, represented two sets of three experiments each at closely spaced width-to-depth ratios, illustrating the approach and eventual crossing of such a neutral stability line. Similarly, the photographs in figure 9, plate 5, suggest another neutral stability line for those cells which are too large. These neutral stability lines, shown as solid lines in figure 11, represent the boundary for three-dimensional instability. Based on the reproducibility of the data, experimental uncertainty connected with these curves appears to be quite small.

The tendency for moderately sized cells to undergo gradual size changes could be interpreted as a two-dimensional instability. This suggests that a second neutral stability curve existed as the dividing line between those cells which exhibited size adjustments and those which did not. Since the average roll

size at the end of long test runs falls within a given band-width, one might be tempted to take this band-width, shown as the heavily shaded region, as the stable band-width. Unfortunately, cells almost never appeared as perfectly parallel rolls at the end of such long runs. Considerable scatter existed among the individual cell sizes even in the same experiment. The spread of these cells is shown as the lightly shaded region. It is clear then that the heavily shaded region cannot be taken as a quantitative measure of the stable band-width. A more quantitative investigation of this problem is not within the capabilities of the present apparatus.

In some tests, it was found that the three-dimensional disturbance will grow for a few hours, then gradually recede and disappear. Closer examination of the photographs reveals the cause for this phenomenon. While the three-dimensional disturbances were developing, the roll cells invariably underwent simultaneous size adjustment toward the stable region. If the time constant for the three-dimensional instability was longer than the time required for the roll cell size to cross the neutral stability line, the three-dimensional instabilities would grow for a while, and then recede after the cell size has crossed the neutral curve.

4. Discussions

The observation described above can be briefly summarized as follows.

(i) It is shown that for the conditions employed ($P_r \approx 1000$, $\Delta\nu/\nu_m \approx 0{\cdot}05$) two-dimensional cells (rolls) were apparently stable within the Rayleigh number range $R_c \leqslant R \leqslant 2{\cdot}5R_c$ provided their width–depth ratios were within a narrow range in the neighbourhood of 1·1.

(ii) When the width–depth ratios were outside this range, the cells would show strong tendencies to adjust their sizes gradually toward the preferred value. These cell size adjustments can be considered basically two-dimensional, in the sense that the flow did not appear to show significant variations in the longitudinal direction.

(iii) When the width–depth ratios were excessively large or excessively small, three-dimensional instabilities appeared in the form of cell boundary distortions and transverse secondary cells.

The fact that the two-dimensional roll cells are stable over the investigated Rayleigh number range is in agreement with recent theoretical predictions (Segel 1965) that roll cells may be stable down to a Rayleigh number $R_l = R_c(1+\epsilon)$, where ϵ is of the order $(\Delta\nu/\nu_m)^2$. In terms of the viscosity variations in the present experiments, R_l is practically indistinguishable from R_c. In this respect the present result also corroborated the experiment of Koschmieder (1966), but is less subjected to the latter's wall effects, which completely dominated his observed structure.

One of the surprising aspects of the results was the strong cell size adjustment tendencies possessed by the flow. It is all the more amazing if one considers that in the process of shrinking or expansion, the flow must generate new cells or suppress old ones near the horizontal boundary. Thus, one may conclude that, for flows of this type, history plays a rather minor role in determining the final flow field, except maybe in the orientation of the rolls.

The fact that the stable band-width is relatively narrow and lies in the vicinity of the critical wave-number is of some practical interest. Since the heat transfer rate is known to be rather insensitive to the horizontal wave-number (Veronis 1966), it would seem that good heat transfer estimates can be made without precise knowledge of the wave-number of the finite-amplitude flow. The critical wave-number from the linear theory could be used as a good first approximation. Whether this is also true for larger Rayleigh numbers or for more complex interchange instability problems remains an interesting problem for future investigations.

The gradual size adjustments of the moderately sized cells is also of interest. In other words, the prevailing form of modal transition for these cells is from a mode k to an immediately adjacent mode $k+\delta k$ rather than to the higher harmonics $2k, 3k, 4k, \ldots$, etc. This finding may be of considerable theoretical interest, since many techniques are currently being developed based on expansions involving a finite number of the $2k$, $3k$, $4k$, ... modes.

In some respects our experiments probably could have been carried out better with a rectangular horizontal configuration, rather than a round one. Indeed, if the width of the apparatus is made adjustable so as to be more compatible with an integral multiple of the basic cell size, one might be able to refine the observed final band-width (i.e. the heavily shaded region in figure 11). However, it must be said that, by using a circular configuration, we have presented a stronger case for the stability of roll cells, which were able to persist despite the circular shape of the vertical boundary.

Probably as a result of the inherently nonlinear nature, the problem of the band-width of stable finite-amplitude modes does not appear to be widely studied. Schlüter *et al.* (1965) showed that, to the first approximation, the cell size band-width of stable roll cells is proportional to $(R-R_c)$ and bounded from above by λc. This cannot be confirmed by our experiments, since their theoretical results are only valid in a region where our experimental uncertainties are large. However, the experiments show that, as the Rayleigh number increased, the stable cell size tended to be slightly larger; contrary to what one would obtain if the results of Schlüter *et al.*, were extrapolated.

In his numerical solution of finite-amplitude convection, Fromm (1965) used time-dependent equations and started his calculations by assuming stagnant initial conditions with small periodic perturbations. Thus, his 'experiment' was procedurally similar to the one reported here. When perturbations of excessively large wavelength were used, it was found that a higher-order mode ($\lambda_1 = 1/2\lambda_0$) tended to develop at the expense of the introduced perturbations, similar to our findings. Since his computer program divided a fixed width to an integral number of cells, one would presume that he was not equipped to observe cell-size adjustments. His two-dimensional equations were also incapable of yielding information on three-dimensional influences.

At the conclusion of this study the authors became aware of an unpublished report by Busse (1966) which extended the technique of Schlüter *et al.* to higher Rayleigh numbers. It was shown that, for rolls of large wave-numbers, three-dimensional instabilities of wavelengths roughly equal to $2h$ would develop.

For rolls of small wave-numbers, the three-dimensional instability would be of considerably shorter wavelength. While the former was in agreement with our experiments, the latter could not be verified too clearly, due to the lack of regularity in the observed instabilities. In addition his predicted stable band-width of cell sizes centred below unity, while our observed band-width lies above unity.

In this connexion, it should be noted that, although the glass thermal conductivity is finite, its influence on the linear critical cell size $\frac{1}{2}\lambda_c$ and critical Rayleigh number R_c is quite small. An estimate of this can be made by expressing the effect of the finite conductivity boundary in the form of $T/z = \beta T$, where $\beta = \beta(\lambda)$ can be determined explicitly from heat conduction equations. The corrected λ_c and R_c can then be obtained from the computed results of Sparrow, Goldstein & Jonsson (1964). For the experiments with $h = \frac{5}{8}$ in., the corrections in λ_c and R_c amounted only to 2·5 and 0·5 % respectively.

Another question concerning the interpretation of the experiment is whether the stability observations are representative of the basic convective flow or are they peculiar to the way these cells were produced. To answer this question, it is noted that the artificial peturbations are only employed for a brief period in the beginning of the experiment. Therefore, if the cells so produced are stable and can persist unchanged for a period many times the thermal time constant of the fluid layer, the flow would most likely be indistinguishable from the steady-state flow corresponding to the same cell size but without any non-uniform heating. In other words, the cell evolution observations on the stable side of the neutral stability line can be accepted as genuine. Similarly, the observations on the unstable side of the neutral stability line can also be accepted as genuine, as long as the time constant of the particular mode of instability concerned is long relative to the time necessary to reach steady state. Here, of course, we interpret steady state as referring to every possible mode with the exception of the unstable mode under consideration. In conclusion, since the observations can be considered valid in a continuous region which includes the stable region and slightly beyond the neutral stability line on the unstable region, the neutral stability line thus obtained can be considered valid.

It is noted that, due to the large Prandtl number and the low Rayleigh number employed, the flow is primarily Stokesian, with negligible inertial terms. The only nonlinear influence of consequence is the $u.\nabla T$ term, and hydrodynamic instabilities involving inertia do not exist. The observations reported here are thus relevant to the elementary interchange stability problem. It would be interesting to inquire whether similar phenomena also exist in other types of interchange instability problems.

Since relevant thermal depths in geophysical flows are rarely constant, the width–depth ratio may scan large ranges. One is thus tempted to find parallelism between such flows and the phenomena observed here. For example, the original convection roll cells in an unstable layer in the atmosphere are likely to have widths comparable to the unstable layer thickness. If subsequent heat transfer or other agents increases the depth of this layer, the cell widths will become too small relative to the layer depth, and thus may develop instabilities similar to

those observed here. One might inquire if this could be the cause of the rectangular matrix sometimes associated with cloud structures. Geophysical flows are of course, extremely complex, and exact comparison is difficult to make. It is merely hoped that these observations may contribute to both the speculative and investigative effort in the field.

The authors wish to express their gratitude to Professors R. Kulsrud and G. Veronis for their careful reading of the manuscript and their valuable suggestions. The study was supported by the National Science Foundation.

REFERENCES

BÉNARD, H. 1901. Les Tourbillons cellulaires dans une nappe liquide transportant de la chaleur par convection en régime permanent. *Ann. Chim. Phys.* **23**, 62–144.

BUSSE, F. 1966 On the stability of two-dimensional convection in a layer heated from below. Unpublished report.

CHANDRASEKHAR, S. 1961 *Hydrodynamic and Hydromagnetic Stability.* Oxford: Clarendon Press.

CHEN, M. M. 1966 Experimental investigation of artificially initiated convective cells. *Bull. Am. Phys. Soc.* **11**, 617.

FROMM, J. E. 1965 Numerical solutions of the non-linear equations for a heated fluid layer. *Phys. Fluids*, **8**, 1757.

KOSCHMIEDER, E. L. 1966 On convection on a uniformly heated plane. *Beit. Z. Phys. d. Atmos.* **39**, 1.

KRISHNAMURTI, R. E. 1967 Thermal convection in a horizontal layer with changing mean temperature. *Bull. Am. Phys. Soc.* **12**, 847, also Ph.D. thesis, University of California, Los Angeles, Calif.

KUO, H. L. 1961 Solution of the non-linear equations of motion of cellular convection and heat transport. *J. Fluid Mech.* **10**, 611–634.

MALKUS & VERONIS 1958. Finite amplitude cellular convection. *J. Fuid Mech.* **4**, 225.

SCHLÜTER, A., LORTZ, D. & BUSSE, F. 1965 On the stability of finite amplitude convection. *J. Fluid Mech.* **23**, 129–144.

SCHMIDT, R. J. & MILVERTON, S. W. 1935 On the stability of a fluid when heated from below. *Proc. Roy. Soc.* A **152**, 586–594.

SEGEL, L. A. 1965 The non-linear interaction of a finite number of disturbances to a layer of fluid heated from below. *J. Fluid Mech.* **21**, 359–384.

SPARROW, E. M., GOLDSTEIN, R. J. & JONSSON, V. K. 1964 Thermal instability in a horizontal fluid layer; effect of boundary conditions and non-linear temperature profile. *J. Fluid Mech.* **18**, 513–528.

VERONIS, G. 1966 Large amplitude Bénard convection. *J. Fluid Mech.* **26**, 49–68.

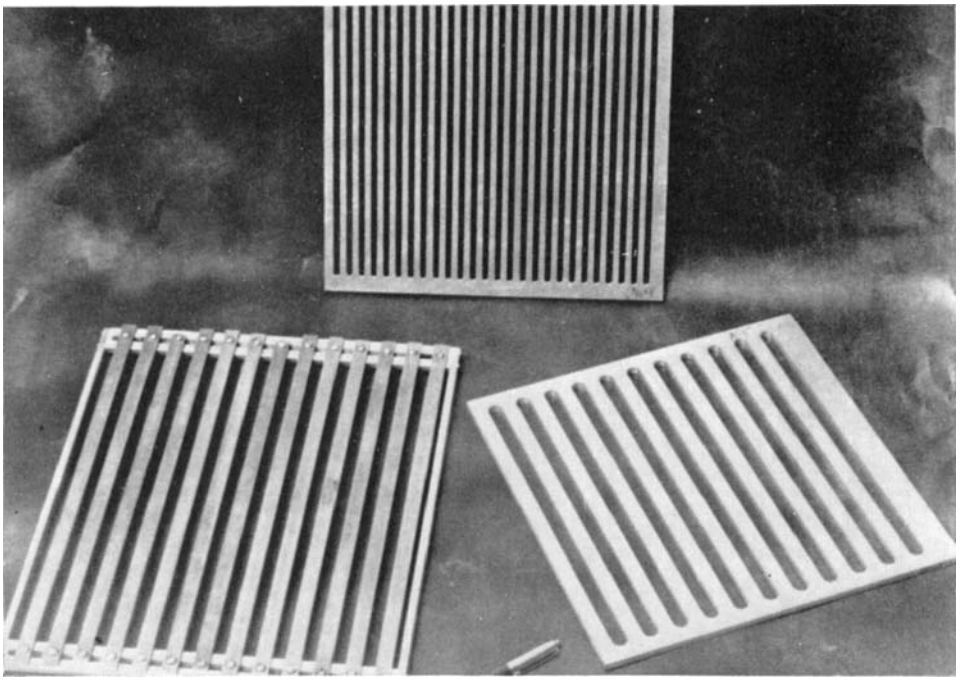

FIGURE 2. Gratings used to excite cells of desired widths.

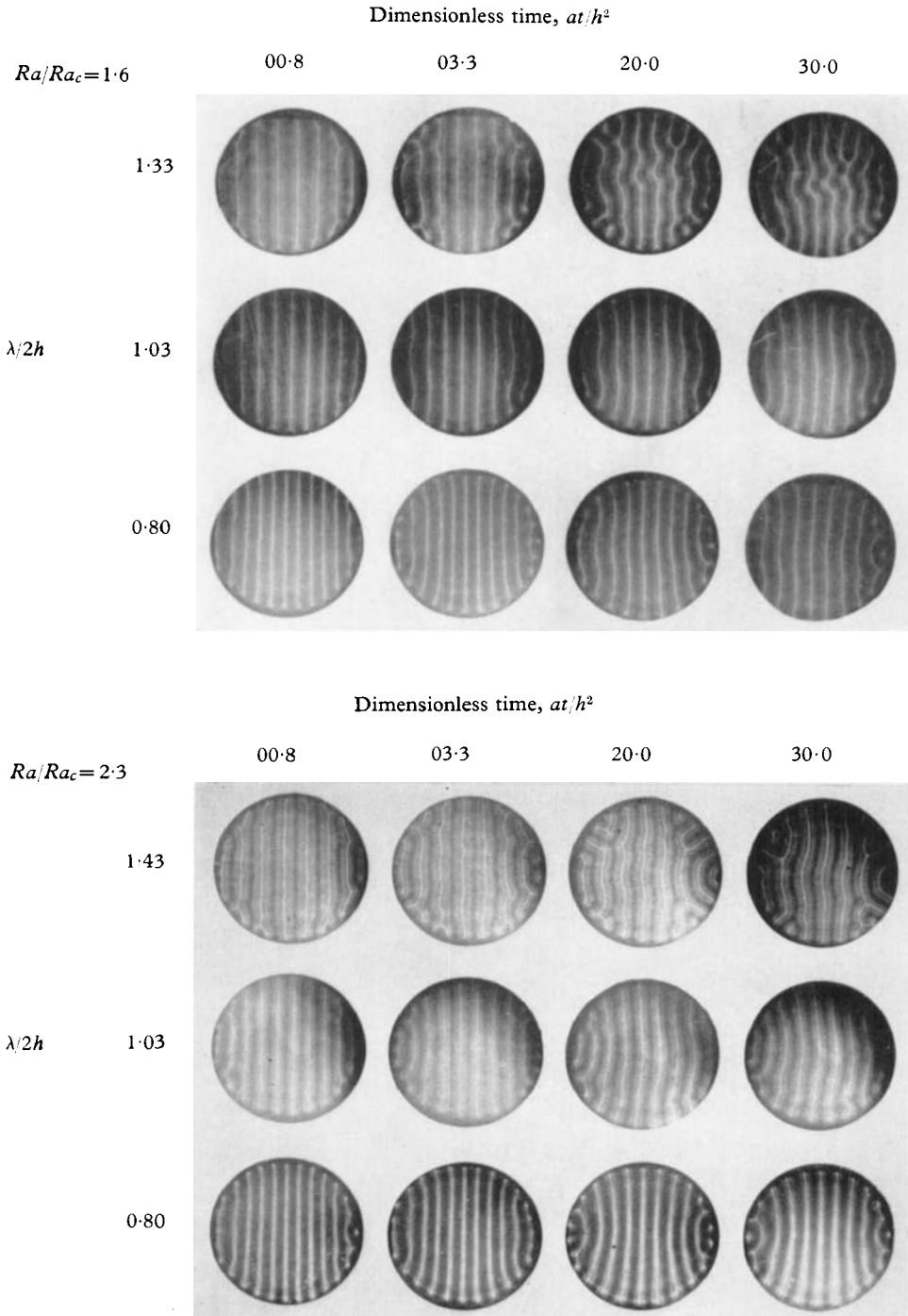

FIGURE 5. Evolution or roll cells of moderate width–depth ratios. Here h denotes the depth and λ corresponds to the width of a single cell.

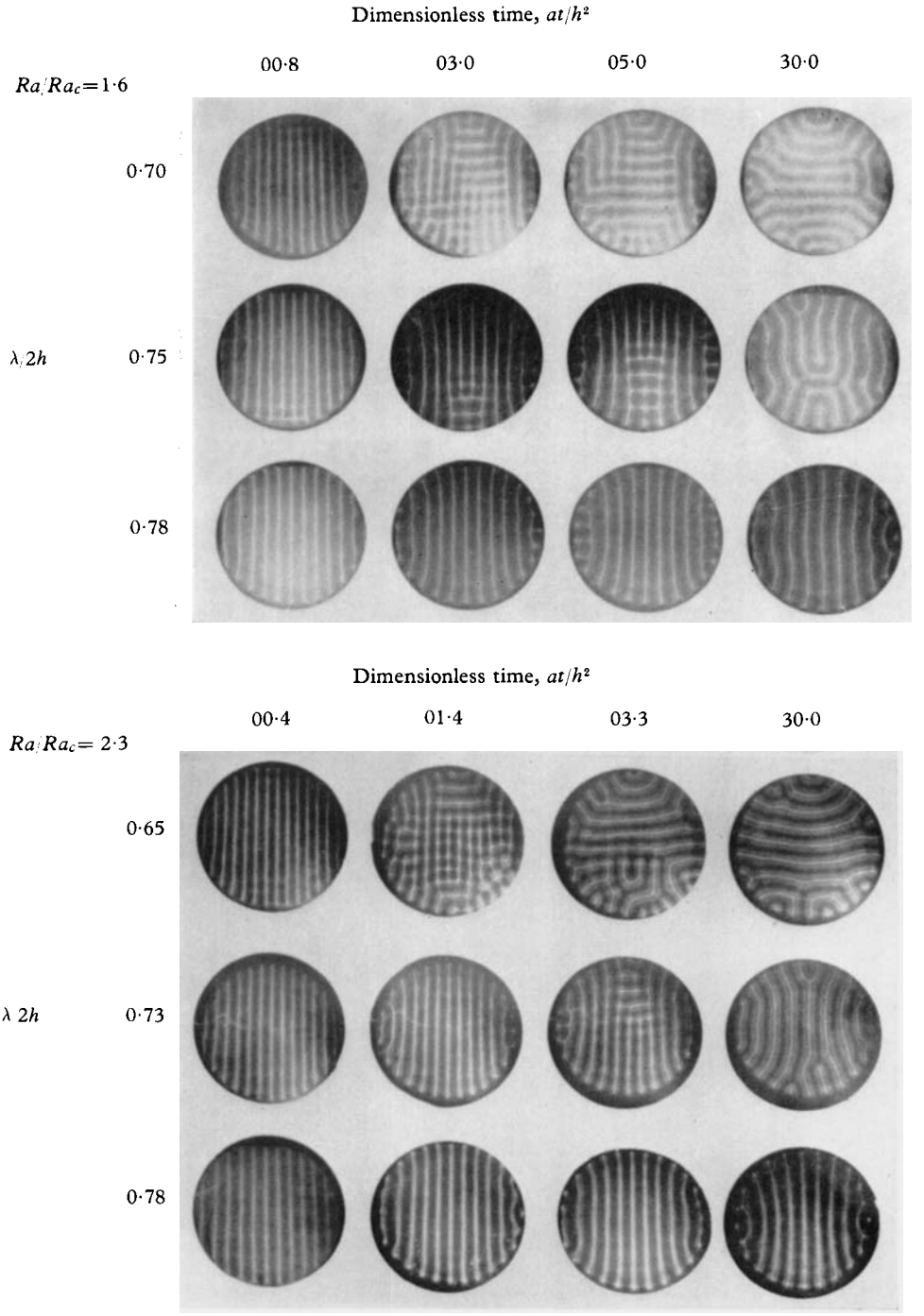

FIGURE 7. Evolution of roll cells with excessively small width–depth ratios.

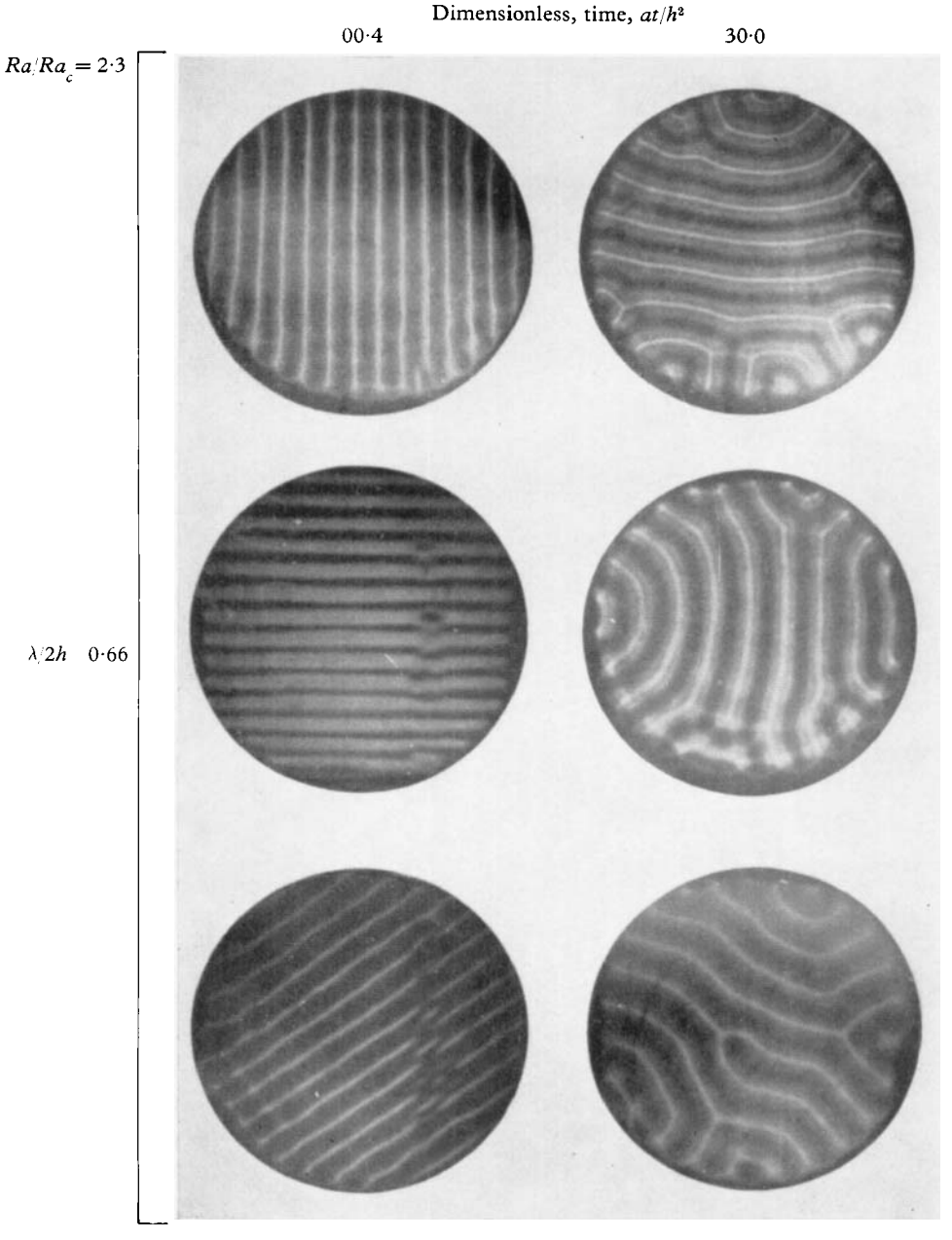

FIGURE 8. Metamorphosis of variously oriented roll cells of small width–depth ratios.

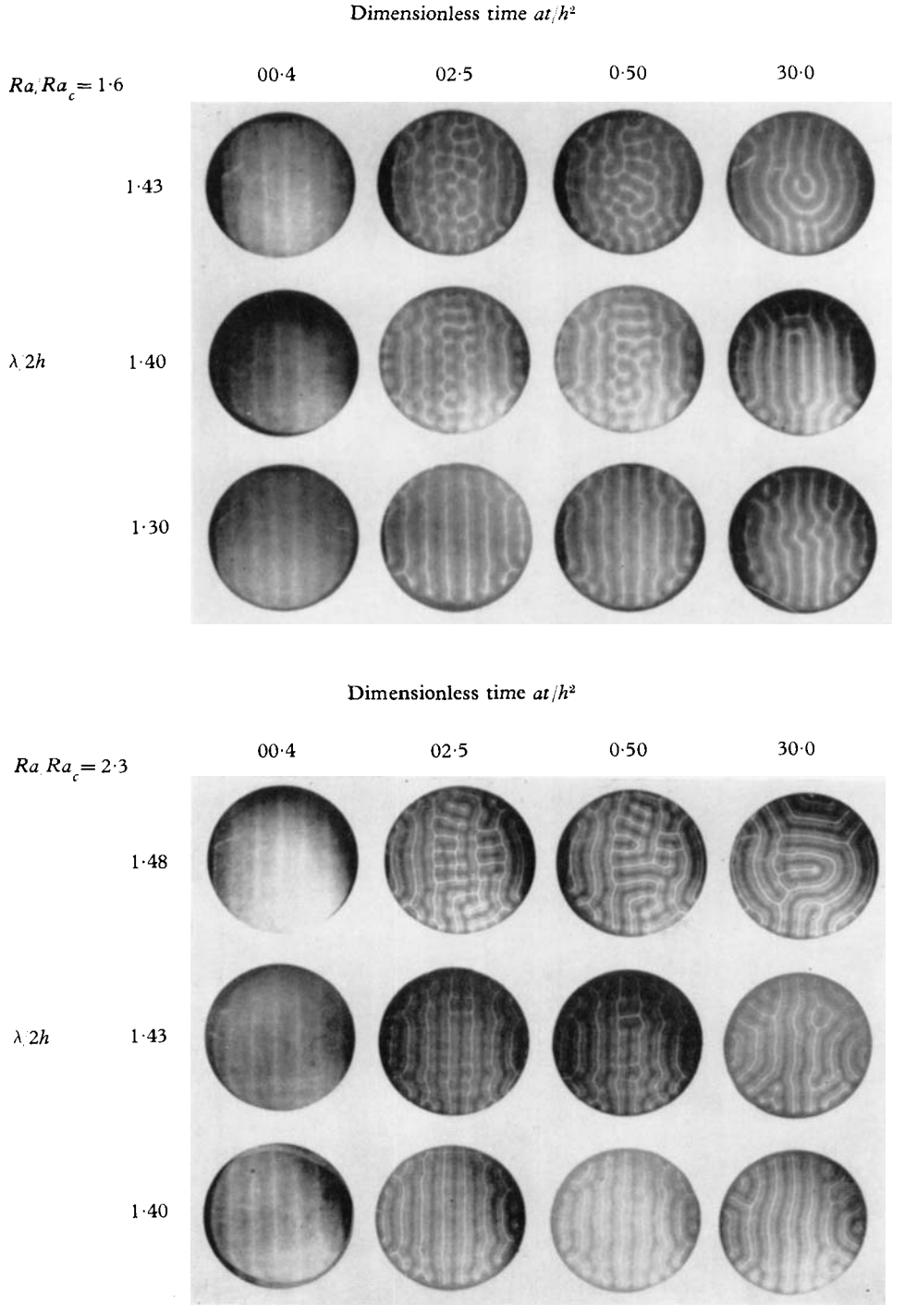

FIGURE 9. Evolution of roll cells with excessively large width–depth ratios.

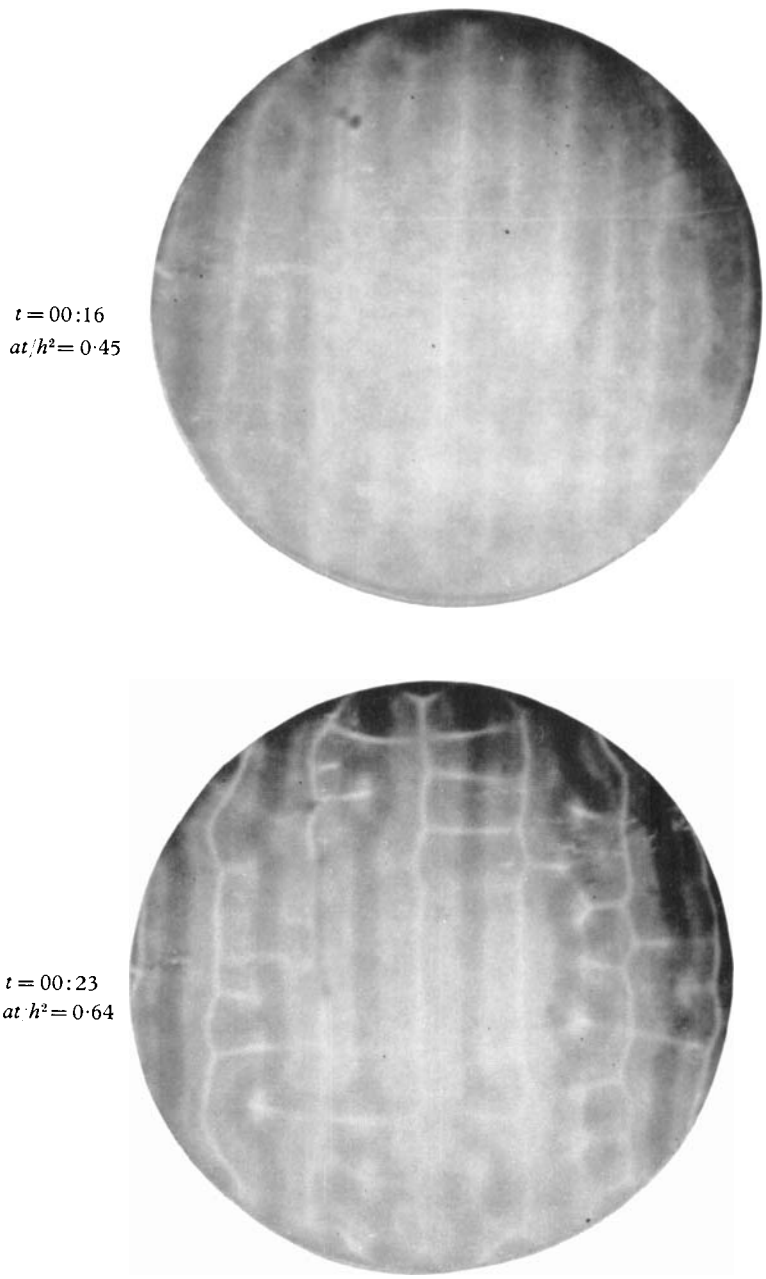

FIGURE 10. Photograph showing second harmonic developing in roll cells of large width-to-depth ratios and the subsequent cross-cells.